Available online at www.sciencedirect.com

ScienceDirect

Energy Procedia 39 (2013) 12 – 19

Energy Procedia

Asian Nuclear Prospects 2012

(ANUP2012)

Parameter Sensitivity Analysis on Pressure Drop of Gas-Solid Flow for Absorber Sphere Pneumatic Conveying

LI Tianjin*, CHEN Feng, QI Weiwei, HUANG Zhiyong, BO Hanliang

Institute of Nuclear and New Energy Technology, Tsinghua University, Beijing 100084, China

Abstract

The pressure drop of gas-solid flow for absorber sphere pneumatic conveying is important for the design and operation of the gas circulator. The simplified one-dimension model is introduced to predict the pressure drop of gas-solid flow for absorber sphere pneumatic conveying. The pressure drop of gas-solid flow in the vertical pipe is the main component part of the total gas-solid flow for absorber sphere conveying. The pressure drop of gas-solid flow for absorber sphere conveying in the vertical pipe with the inside diameter 47 mm and conveying height 23 m is predicted by the simplified model. The superficial gas velocity considered is in the range of 1.5 to 3.0 times of the terminal velocity of a single particle. The solid mass flow rate considered is in the range of 0.2 to 1.2 kg/s. Particle velocity, solid friction factor and solid mass flow rate are important parameters to predict pressure drop of vertical pipe. The typical empirical correlations of particle velocity and solid friction factor reported in the literature are adopted to predict the pressure drop of vertical pipe. The superficial gas velocity for absorber sphere conveying is suggested to be two times of the terminal velocity of a single particle. For the suggested superficial gas velocity, the predicted pressure drop of vertical pipe by using empirical correlations is in the range of 15 to 20 kPa and 31 to 50 kPa for solid mass flow rate at 0.2 kg/s and 1.2 kg/s, respectively. For the suggested superficial gas velocity, the relatively conservative predicted pressure drop of vertical pipe is in the range of 20 to 78 kPa for solid mass flow rate in the range of 0.2 to 1.2 kg/s. Further work is needed to verify the pressure drop model and to modify the key parameters for absorber sphere conveying in helium.

Keywords: pressure drop; *vertical pipe*; *gas-solid flow*; *pneumatic conveying*; *high-temperature gas-cooled reactor*

* Corresponding author. Tel.: +86-10-89796051; fax: +86-10-62797615.
E-mail address: tjli@tsinghua.edu.cn.

doi:10.1016/j.egypro.2013.07.187

1. Introduction

The high-temperature gas-cooled reactor (HTR or HTGR) has many advantages, e.g. the inherent safety, high efficiency, potential application for process steam [1-10]. Two independent shutdown systems, i.e. the control rod system and the absorber sphere shutdown system, are designed for shutdown purposes. The absorber sphere (B_4C in graphite) is designed to drop into the reflector borings by its own gravity [1, 11]. The absorber sphere in the reflector borings is needed to be transported back to the sphere storage vessel by pneumatic conveying when the reactor is needed to be started up [11-14].

The pressure drop of the gas-solid flow for the absorber sphere pneumatic conveying is important for designing the gas circulator. The diameter and the particle density of the absorber sphere is 6.0 mm and 1800 kg/m^3, respectively. These particles were Geldart type-D particles [15]. The conveying gas is helium at some temperature and high pressure. The inside diameter and vertical height of the conveying pipe is 47 mm and approx. 23 m, respectively. The absorber sphere conveying in helium is a special application of pneumatic conveying technique, which is different from the traditional air conveying application.

The conveying characteristics of 6.0 mm glass sphere in ambient air have been investigated in our previous work [16-20]. The experimental result showed that the gas-solid flow in the vertical pipe was dilute phase conveying. The schematic diagram of the experimental setup is shown in Fig. 1. The particle density of the glass spheres used in the experiments was 2518 kg/m^3, which is different from that of the absorber sphere. The vertical height of the conveying line was 10.66 m. Detailed description of the experimental setup are reported elsewhere [16].

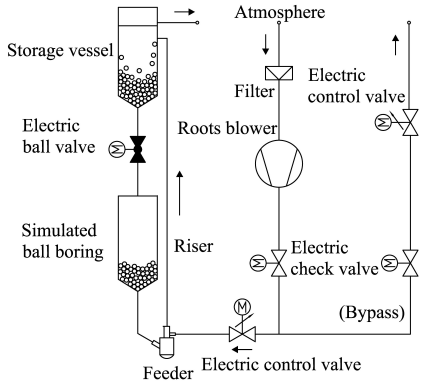

Fig. 1. Experimental setup in the previous work for conveying 6.0 mm glass spheres in ambient air

Table 1 The main data used to predict Δp_{vt} for absorber sphere conveying

Parameter	*Value*
gas	helium
solid	absorber sphere
ρ_g	6.33 kg/m^3
f_g	0.024
D	47 mm
h	23 m
d_s	6.0 mm
ρ_s	1800 kg/m^3
G_s	0.2 to 1.2 kg/s
u_t	7.14 m/s
u_g/u_t	1.5 to 3.0

The aim of this study is to make a further understanding of the absorber sphere pneumatic conveying. The simplified one-dimension model for predicting gas-solid flow pressure drop is introduced for absorber sphere conveying. The typical empirical correlations reported in the literature for the important parameters in the model are investigated. The predicted pressure drop of the dilute phase gas-solid vertical flow at different absorber sphere mass flow rate is reported.

2. Pressure drop of gas-solid flow

Considerable theoretical and experimental work has been devoted to predict the pressure drop in a gas-solid flow in pipes, but the reliable general model has not yet been developed [15]. The one-dimension model is usually used to predict gas-solid flow pressure drop [15, 21], which can be mainly described by

Eq. 1. The simplified one-dimension model is used to predict pressure drop of absorber sphere conveying. It is assumed that particle acceleration is approximately completed at the outlet of the feeder. Eq. 2 is used to predict the pressure drop of gas-solid flow for absorber sphere conveying, since the pressure drop of cyclone and the short horizontal conveying pipe are negligible. The pressure gradient of bend in the conveying line is assumed to be proportional to the pressure gradient of the vertical pipe. Eq. 2 to Eq. 8 is the main equations of the simplified model for predicting pressure drop of gas-solid flow for absorber sphere conveying in this study.

The additional pressure drop due to solid in the pipe is mainly affected by K_{fd}, K_b, u_s and f_s in the simplified model. K_{fd} is in the range of 0.17 to 0.37 in the previous experimental work with 6.0 mm glass sphere conveying in ambient air [20]. The maximum K_b is approx. 3.5 in the experimental work with 1.8 mm ceramic sphere conveying in ambient air [21]. The additional pressure drop due to solid in the vertical pipe is the main part of the absorber sphere gas-solid flow pressure drop. f_s and u_s are important parameters to determine the key parameter λ_z for predicting Δp_{vt}.

$$\Delta p_{gs} = \Delta p_g + \Delta p_s = \Delta p_g + \Delta p_A + \Delta p_{s(vt)} + \Delta p_{s(hr)} + \Delta p_b + \Delta p_C \tag{1}$$

$$\Delta p_{gs} \approx \Delta p_{fd} + \Delta p_{vt} + \Delta p_b \tag{2}$$

$$\Delta p_{fd} = \left(1 + \mu K_{fd}\right) \xi_{fd} \rho_g u_g^2 / 2 \tag{3}$$

$$\Delta p_{vt} = \Delta p_{g(vt)} + \Delta p_{s(vt)} = \varepsilon \rho_g g h + f_g \varepsilon \rho_g u_g^2 h / (2D) + (1-\varepsilon) \rho_s g h + f_s (1-\varepsilon) \rho_s u_s^2 h / (2D) \tag{4}$$

$$\Delta p_{s(vt)} = (1-\varepsilon) \rho_s g h + f_s (1-\varepsilon) \rho_s u_s^2 h / (2D) = \mu \lambda_z \rho_g u_g^2 h / (2D) \tag{5}$$

$$\mu = G_s / \left(\rho_g u_g \pi D^2 / 4\right) = \rho_s (1-\varepsilon) u_s \pi D^2 / 4 / \left(\rho_g u_g \pi D^2 / 4\right) = \rho_s (1-\varepsilon) u_s / \left(\rho_g u_g\right) \tag{6}$$

$$\lambda_z = f_s \frac{u_s}{u_g} + \frac{2}{\left(u_s / u_g\right)\left(u_g / \sqrt{gD}\right)^2} \tag{7}$$

$$\Delta p_b = K_b L_b \Delta p_{vt} / h \tag{8}$$

Sankar et al [22] reported the u_s correlation Eq. 9 by fitting a large number of experimental data reported in the literature. This u_s correlation proved to be suitable for application in dilute phase vertical conveying of spherical ceramic particles of 1.8 mm diameter with air in a 50 mm i.d. pipe [21]. The drag coefficient on a group of particles may be different from that on a single particle. Considering this effect, another u_s correlation [23], i.e. Eq. 10, is also considered in this study.

The correlation for f_s was review by Yang [24]. The classic f_s correlations were suggested based on fitting of experimental data reported in the literature. The coefficient of f_s correlation by Yang was revised by Garic et al [25] based on the experimental data for conveying spherical glass particles of 1.20, 1.94 and 2.98 mm diameter with air in a 30 mm i.d. glass pipe. The typical f_s correlations are summarized in Table 2. Eq. 14 is the revised one of Eq. 13 by Yang [24].

$$u_s = u_g / \varepsilon - 0.011 \mu^{-0.1} u_t^{-0.34} \left(d_s / D\right)^{0.56} \left(\rho_g / \rho_s\right)^{-0.68} \left(u_g / \varepsilon\right)^{1.34} \tag{9}$$

$$u_s = u_g / \varepsilon - u_t \varepsilon^{2.17} \tag{10}$$

$$\varepsilon = 1 - 4 G_s / \left(\pi \rho_s u_s D^2\right) \tag{11}$$

$$u_t = 1.75 \sqrt{d_s g \left(\rho_s - \rho_g\right) / \rho_g} \tag{12}$$

The main data used to predict Δp_{vt} for absorber sphere conveying in this study are listed in Table 1. For the given G_s and u_g, the predicted Δp_{vt} is obtained by using the corresponding f_s and u_s correlations. The process for calculating Δp_{vt} using the u_s correlation of Sankar et al [18] is as follows:

- Calculate μ with Eq. 6.
- Iterate to get u_s and ε with Eq. 9 and Eq. 11.
- Calculate f_s with correlation Eq. 14 and Eq. 16.
- Calculate the corresponding Δp_{vt} with Eq. 4.

Table 2 Typical f_s correlations reported in the literature

Reference	f_s correlations	
Yang [24]	$f_s = 0.0206(1-\varepsilon)/\varepsilon^3\left[u_t(1-\varepsilon)/(u_g/\varepsilon - u_s)\right]^{-0.869}$	(13)
Yang [24]	$f_s = 0.0126(1-\varepsilon)/\varepsilon^3\left[u_t(1-\varepsilon)/(u_g/\varepsilon - u_s)\right]^{-0.979} \quad \left(\frac{u_g/\varepsilon}{u_t} > 1.5\right)$	(14)
Yang [24]	$f_s = 0.041(1-\varepsilon)/\varepsilon^3\left[u_t(1-\varepsilon)/(u_g/\varepsilon - u_s)\right]^{-1.021} \quad \left(\frac{u_g/\varepsilon}{u_t} > 1.5\right)$	(15)
Garić [25]	$f_s = 0.0068(1-\varepsilon)/\varepsilon^3 \frac{u_t}{u_g}\left[u_t(1-\varepsilon)/(u_g/\varepsilon - u_s)\right]^{-1.5}$	(16)

3. Results and discussion

Fig. 2 shows the typical result of the calculated u_s at different u_g/u_t and G_s. The calculated u_s from Eq. 9 is much larger than that of Eq. 10. With the increase of u_g/u_t from 1.5 to 3.0, the difference of the calculated u_s between Eq. 9 and Eq. 10 decrease from approx. 4.7 m/s to approx. 2.2 m/s. The calculated u_s increase slightly with increase of G_s from 0.2 kg/s to 0.8 kg/s for both Eq. 9 and Eq. 10, respectively.

Fig. 3 shows the typical result of the calculated f_s at different u_g/u_t. The corresponding G_s is 0.4 kg/s. The calculated f_s from Eq. 16 by using u_s correlation Eq. 10 is approx. 0.026, which is the maximum of the four calculated f_s. The minimum of the calculated f_s from Eq. 14 by using u_s correlation Eq. 9 is in the range of 0.003 to 0.008. It can be concluded that the difference of the calculated f_s by different correlations is large. The calculated f_s by using u_s correlation Eq. 10 is approximately constant with u_g/u_t in the range of 1.5 to 3.0. The calculated f_s by using u_s correlation Eq. 9 increase with the increase of u_g/u_t. The calculated f_s from Eq. 16 is larger than that of Eq. 14 by using the same u_s correlation.

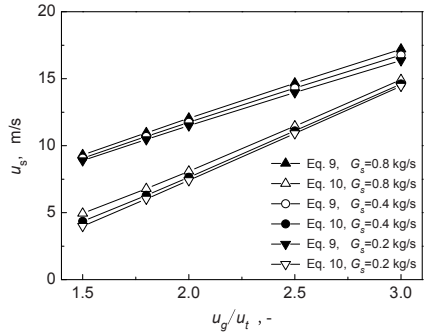

Fig. 2. Typical result of calculated u_s at different u_g/u_t and G_s

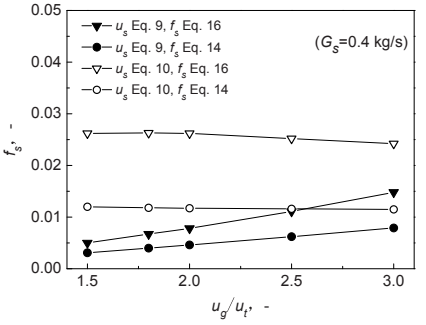

Fig. 3. Typical result of calculated f_s at different u_g/u_t (G_s = 0.4 kg/s)

Fig. 4 shows the result of the predicted Δp_{vt} changing with u_g/u_t for different G_s. The predicted Δp_{vt} from u_s correlation Eq. 10 and f_s correlation Eq. 16 is the maximum for the certain u_g/u_t and G_s. This is mainly attributed to the characteristics of f_s, which is shown in Fig. 3 with G_s = 0.4 kg/s as a typical result. The predicted Δp_{vt} from u_s correlation Eq. 10 is usually larger than that from u_s correlation Eq. 9 with the f_s correlation. With u_g/u_t = 2, the predicted Δp_{vt} is in the range of 15 to 20 kPa and 31 to 50 kPa for G_s 0.2 kg/s and 1.2 kg/s, respectively. With the same u_s correlation, the difference of the predicted Δp_{vt} from f_s correlation Eq. 14 and Eq. 16 is usually < 10 kPa, which is negligible from the view point of engineering application. This infers that appropriate u_s is quite important for predicting Δp_{vt}.

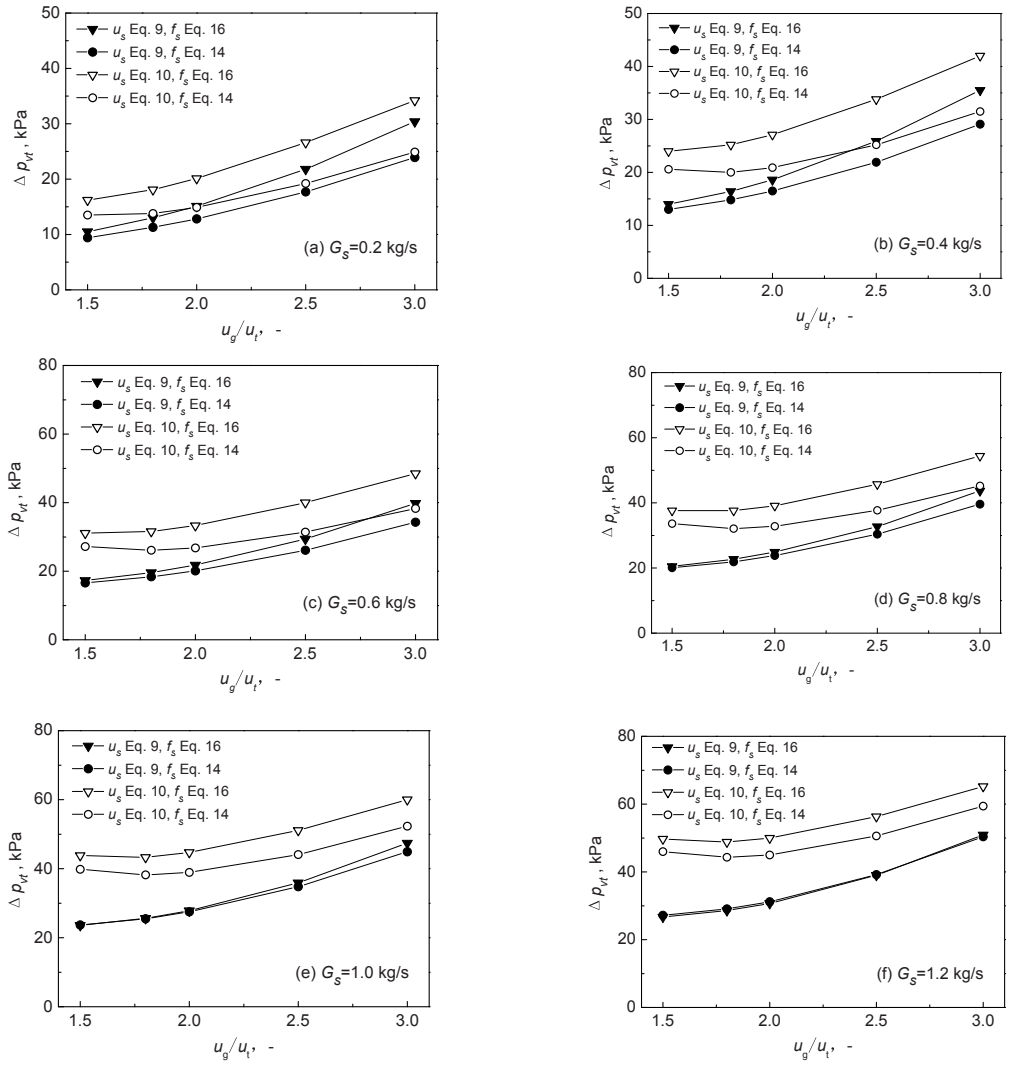

Fig. 4. The predicted Δp_{vt} change with u_g/u_t for different G_s in the range of 0.2 to 1.2 kg/s (u_s correlation Eq. 9 and Eq. 10, f_s correlation Eq. 14 and Eq. 16)

It can be deduced from Eq. 4 that λ_z increase with the increase of u_s when $u_s > \sqrt{2gD/f_s}$ for a given u_g. The previous experimental work for conveying 6.0 mm glass sphere with ambient air showed that f_s remained approx. 0.027 for $u_g/u_t > 1.3$ [19]. Given $f_s = 0.027$, the value of $\sqrt{2gD/f_s}$ will be 5.8 m/s. As shown in Fig. 2, the calculated u_s from Eq. 9 is much larger than that of Eq. 10. u_s is > 5.8 m/s when $u_g/u_t > 1.8$. Therefore, u_s correlation Eq. 9 is used to give a relatively conservative prediction for Δp_{vt} considering the engineering application.

Fig. 5 shows the result of the predicted Δp_{vt} with the given $f_s = 0.027$ and u_s correlation Eq. 9 changing with u_g/u_t for different G_s. The predicted Δp_{vt} is in the range of 15 to 33 kPa and 65 to 107 kPa for G_s 0.2 kg/s and 1.2 kg/s, respectively. The predicted Δp_{vt} is in the range of 20 to 78 kPa for G_s in the range of 0.2 to 1.2 kg/s and $u_g/u_t = 2$.

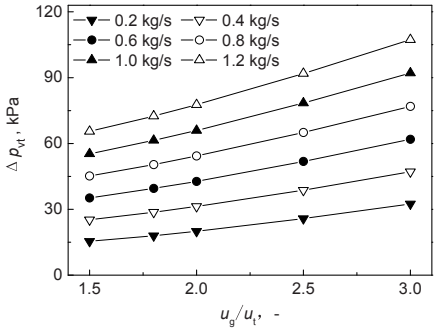

Fig. 5. The predicted Δp_{vt} change with u_g/u_t for different G_s in the range of 0.2 to 1.2 kg/s (f_s = 0.027 and u_s correlation Eq. 9)

The absorber sphere is made of B_4C mixed in graphite, which will contribute to the reactivity control. The allowable G_s is affected by reactor physics. Furthermore, it is suggested that G_s should be within a reasonable level from the view point of gas-solid flow characteristics. If G_s is too high to result in a high enough pressure drop for absorber sphere conveying, difficulty may be encountered for choosing and operating the gas circulator.

u_g is an important parameter for the operating of absorber sphere conveying. Considering the predicted result of Δp_{vt} and the gas-solid flow theories, it is suggested that $u_g/u_t = 2$ for the operating of absorber sphere pneumatic conveying.

Experimental work will be done in the near future to verify these results.

4. Conclusion

The absorber sphere conveying in high pressure helium is a special application of pneumatic conveying technique, which is different from the traditional air conveying application. The simplified one-dimension model is used to predict the pressure drop of gas-solid flow for absorber sphere conveying. The pressure drop of gas-solid flow in the vertical pipe is the main component part of the total gas-solid flow for absorber sphere conveying. The typical empirical correlations of particle velocity and solid friction factor reported in the literature are used to predict the additional pressure drop of vertical pipe due to solid particles. The u_g/u_t and G_s considered in this study is in the range of 1.5 to 3.0 and 0.2 to1.2 kg/s, respectively. $u_g/u_t = 2$ is suggested for the operating of absorber sphere pneumatic conveying. With u_g/u_t = 2, the predicted Δp_{vt} by using empirical correlations is in the range of 15 to 20 kPa and 31 to 50 kPa for G_s 0.2 kg/s and 1.2 kg/s, respectively. A relatively conservative predicted pressure drop of vertical pipe is conducted by using $f_s = 0.027$ from our previous cold state experimental work and u_s correlation Eq. 9. The corresponding predicted Δp_{vt} is in the range of 15 to 33 kPa and 65 to 107 kPa for G_s 0.2 kg/s and 1.2 kg/s, respectively. The relatively conservative predicted Δp_{vt} is in the range of 20 to 78 kPa for G_s in the range of 0.2 to 1.2 kg/s and $u_g/u_t = 2$.

Further experimental work is needed to verify the simplified pressure drop model and to modify the key factors. The full scale experimental setup is being constructed to investigate the pneumatic conveying characteristics of the absorber spheres in helium.

Nomenclature

d_s	particle diameter
D	inside diameter of conveying pipe
f_g	gas friction factor
f_s	solid friction factor
g	gravitational acceleration
h	conveying height, m
K_b	pressure drop factor of the bend due to gas-solid flow
K_{fd}	additional pressure drop factor of the feeder due to solid particles
L_b	spread length of bend
u_g	superficial gas velocity based on empty pipe cross section
u_s	actual particle velocity
u_t	terminal velocity of a single particle
G_s	solid mass flow rate
ε	voidage
μ	mass flow ratio of solid and gas
ξ_{fd}	pressure drop factor of feeder due to gas
ρ_g	gas density
ρ_s	particle density
λ_z	additional pressure drop factor in a pipe due to solids in a flowing stream
Δp_{gs}	total pressure drop of the gas-solid flow pipe line
Δp_g	pressure drop due to gas
Δp_s	additional pressure drop due to solid particles
Δp_{vt}	pressure drop of vertical pipe
$\Delta p_{g\,(vt)}$	pressure drop of vertical pipe due to gas
$\Delta p_{s\,(vt)}$	additional pressure drop of vertical pipe due to solid particles
Δp_{fd}	pressure drop of particle feeder
Δp_b	pressure drop of bend
Δp_A	pressure drop due to acceleration of solid particles
$\Delta p_{s\,(hz)}$	additional pressure drop of horizontal pipe due to solid particles
Δp_C	pressure drop of cyclone

Acknowledgements

The work is supported by the National S&T Major Project (Grant No. ZX06901).

References

[1] Zhang ZY, Wu ZX, Wang DZ, Xu YH, Sun YL, Li F, Dong YJ. Current status and technical description of Chinese 2×250 MWth HTR-PM demonstration plant. *Nuclear Engineering and Design* 2009; **239**: 1212–1219.

[2] Wu ZX, Lin DC, Zhong DX. The design features of the HTR-10. *Nuclear Engineering and Design* 2002; **218**: 25–32.

[3] Lohnert GH, Reutler H. The modular HTR—a new design of high-temperature pebble-bed reactor. *Nuclear Energy*1983; **22**: 197–200.

[4] Reutler H, Lohnert GH. Advantages of going modular in HTRs. *Nuclear Engineering and Design*1984; **78**: 129–136.

[5] Lohnert GH.. Technical design features and essential safety-related properties of the HTR-Module. *Nuclear Engineering and Design*1990; **121**: 259–275.

[6] Wu ZX, Zhang ZY. *The advanced nuclear energy system and high temperature gas-cooled reactor*. Beijing: Tsinghua University Press; 2004 (in Chinese).

[7] Zhang ZY, Wu ZX, Sun YL, Li F. Design aspects of the Chinese modular high-temperature gas-cooled reactor HTR-PM. *Nuclear Engineering and Design* 2006; **236**: 485–490.

[8] Zhang ZY, Sun YL. Economic potential of modular reactor nuclear power plants based on the Chinese HTR-PM project. *Nuclear Engineering and Design* 2007; **237**: 2265-2274.

[9] Wu ZX, Yu SY. HTGR projects in China. *Nuclear Engineering and Technology* 2007; **39**: 103-110.

[10] Koster A, Matzner HD, Nicholsi DR. PBMR design for the future. *Nuclear Engineer and Design* 2003; **222**: 231-245.

[11] Zhou HZ, Huang ZY, Diao XZ. Design and verification test of the small absorber ball system of the HTR-10. *Nuclear Engineering and Design* 2002; **218**: 155-162.

[12] Peng MF, Diao XZ, Huang ZY, Zhou HZ. Verif ication test of pneumatic conveying of small absorber ball system for 10 MW high temperature gas-cooled test reactor. *Atomic Energy Science and Technology* (in Chinese) 2003; **37**: 543-547.

[13] Matzner HD. PBMR existing and future R&D test facilities. *The 2nd International Topical Meeting on High Temperature Reactor Technology*, Beijing, China: 2004.

[14] Yang F, Huang ZY, He XD, Zhang P, Li L, Chen F, Analysis and experiment of new style discharge vessel in reserve shutdown system of high-temperature gas-cooled reactor. *Atomic Energy Science and Technology* (in Chinese) 2009; **43**(Suppl.): 297-300.

[15] Klinzing GE, Rizk F, Marcus R, Leung LS. *Pneumatic conveying of solids: A Theoretical and practical approach*. 3rd ed. Springer; 2010.

[16] Chen WS, Li TJ, Chen F, He XD, Luo J, Huang ZY. Experimental study on visualization discharge vessel for pneumatic conveying of absorber spheres. *Atomic Energy Science and Technology* (in Chinese) 2012; **46**(1): 94-98.

[17] Li TJ, Chen F, He XD, Chen WS, Huang ZY. Visualization experimental study on starting process of the absorber sphere pneumatic conveying. In: *The 4th Asia-Pacific Power and Energy Engineering Conference*, Shanghai, China: 2012.

[18] Li TJ, Chen F, He XD, Chen WS, Sun B, Huang ZY. Experimental study of the absorption spheres pile after the interruption and the restart of the pneumatic conveying. *Nuclear Power Engineering* (in Chinese) 2012; **33**(4): 54-57.

[19] Li TJ, Chen F, He XD, Chen WS, Luo J, Huang ZY. Experimental study on the additional pressure drop due to solids in the riser for the pneumatic conveying of the absorber spheres. *Progress Report on China Nuclear Science & Technology* (in Chinese) 2011; **2**(3): 564-570.

[20] Li TJ, Chen F, He XD, Chen WS, Sun B, Huang ZY. Cold test of additional pressure drop due to solid of the feeder for the absorber sphere pneumatic conveying. In: *The 8th new reactor and research reactor national conference* (in Chinese), Xi'an, China: 2012, p. 47-50.

[21] Jing S, Jiang PL, Hu QY, Wang JF, Jin Y. Pressure drop characteristics of vertical dilute-phase gas conveying. *The Chinese Journal of Process Engineering* (in Chinese) 2001; **1**(1): 25-29.

[22] Sankar SR, Smith TN. Slip velocity in pneumatic transport, part 2. *Powder Technology* 1986; **47**: 179-194.

[23] Yang WC. Estimating the solid particle velocity in vertical pneumatic conveying lines. *Ind Eng Chem Fundam* 1973; **12**: 349-352.

[24] Yang WC. A correlation for solid friction factor in vertical pneumatic conveying lines. *AIChE J* 1978; **24**: 548-552.

[25] Garić RV, Grbavčić ŽB, Jovanović SDj. Hydrodynamic modeling of vertical non-accelerating gas-solids flow. *Powder Technology* 1995; **84**: 65-74.